

Conducted EMI of DC–DC Converters With Parametric Uncertainties

Moisés Ferber, Christian Vollaïre, Laurent Krähenbühl, Jean-Louis Coulomb, and João A. Vasconcelos

Abstract—This paper presents a new methodology to analyze the conducted interferences of power converters when its parameters are described by probability density functions rather than numerical values. The methodology is based on determining a set of surrogate models per frequency of the converter, which has less input and output variables, and shorter simulation time but similar precision for the evaluation of conducted emissions. This approach presents several advantages when compared to classical ones, such as Monte Carlo simulations and collocation methods. The results are presented as probability density functions and confidence intervals.

Index Terms—Electromagnetic compatibility, power electronics, probability, uncertainty.

I. INTRODUCTION

THE rapid development of semiconductor technology in the last decades increased significantly the presence of power converters in electric and electronic equipment, such as computer power supplies, voltage converters, electronic ballasts, and variable-speed drives. These converters often use diodes and transistors as switches, in order to control the output voltage of dynamical loads. The switching operation should have the highest possible frequency from a performance point of view, but the fast commutation with high value of di/dt produces conducted electromagnetic interference (EMI) in a vast frequency range.

The conducted interferences are measured with a line impedance stabilization network (LISN) and it should respect certain standards, depending on the country. In power electronics, conducted emission is considered very important [1].

There are several computer tools to model and simulate electronic circuits that can be used for power converters, such as

SPICE, SABER, and MATLAB/Simulink. Instead of constructing a conventional schematic of a converter containing only the nominal values of the circuit elements, one can also include in the model the parasitic effects of the components and tracks, as well as the complex behavior of semiconductor devices. The disadvantage though is the significant increase of the simulation time. In some cases, there can be even convergence problems [2].

Thus, it would be possible to predict the conducted interferences of a given topology of a converter at design phase. This eventually avoids manufacturing a prototype which fails to respect a certain EMC standard, greatly reducing design costs.

However, these computer tools do not take into account the uncertainties of the voltage sources, components, tracks, and parasitic effects. In reality, the nominal value of these parameters is insufficient to describe phenomena such as production dispersion, aging, and temperature and humidity variation. In applications in which these phenomena cannot be neglected, it is necessary to quantify these uncertainties and analyze their impact on the EMI.

The most common method of uncertainty propagation is based on the Monte Carlo (MC) approach and it has been already applied to EMC [3]–[6]. It is appropriate for linear and nonlinear systems with a large number of parameters. It is also very robust and simple to implement. In this paper, we use it as a comparison tool. The main issue about MC is the large number of simulations required to achieve a satisfactory accuracy. An alternative approach based on risk analysis was developed in [7].

Another method that has recently been evaluated in EMC is the unscented transform (UT) in [8] and [9]. A detailed and formal development of this methodology is accessible in [10]. This approach requires considerably less simulations than MC but it provides only the statistical moments of the output, which in most cases are limited to the average and standard deviation. Considering that the output probability density function (PDF) can be any distribution, this method becomes limited. Moreover, the number of simulations required grows rapidly with the number uncertain parameters. In this paper, a converter with 45 parameters will be analyzed, and in this case, the UT is unfeasible.

In this context, we propose a new methodology to analyze nonlinear, time-variant converters with a large number of uncertain parameters described by any PDF in the frequency domain.

II. METHODOLOGY

The methodology consists basically of four simple steps and it may be applied to a general power converter represented by

$$Y = G(X_1, X_2, \dots, X_n, f) \quad (1)$$

Manuscript received March 26, 2012; revised July 12, 2012; accepted December 10, 2012. Date of publication January 9, 2013; date of current version July 22, 2013. This work was supported in part by Agence Nationale de la Recherche, program VTT 2010, projet E-CEM.

M. Ferber is with Laboratoire Ampère, UMR 5005 CNRS, Ecole Centrale de Lyon, Ecully 69134, France, and also with Evolutionary Computing Laboratory, Universidade Federal de Minas Gerais, Pampulha Belo Horizonte, Minas Gerais 31270-901, Brazil (e-mail: moisesferber@gmail.com).

C. Vollaïre is with the Laboratoire Ampère, CNRS UMR5005, Ecole Centrale de Lyon, Ecully 69134, France (e-mail: Christian.Vollaïre@ec-lyon.fr).

L. Krähenbühl is with Centre National de la Recherche Scientifique, Paris, France, and also with Laboratoire Ampère, CNRS UMR5005, Ecole Centrale de Lyon, Ecully 69134, France (e-mail: Laurent.Krahenbuhl@ec-lyon.fr).

J.-L. Coulomb is with G2ELab, CNRS UMR5269, Ecole Nationale Supérieure d'Ingénieurs pour l'Energie, l'Eau et l'Environnement, Grenoble Institute of Technology, Grenoble 38000, France (e-mail: Jean-louis.Coulomb@g2elab.grenoble-inp.fr).

J. A. Vasconcelos is with the Evolutionary Computing Laboratory, Universidade Federal de Minas Gerais, Belo Horizonte 31270-901, Brazil (e-mail: joao@cpdee.ufmg.br).

Color versions of one or more of the figures in this paper are available online at <http://ieeexplore.ieee.org>.

Digital Object Identifier 10.1109/TEM.2012.2235443

where

Y is the conducted interference in the frequency domain. It can be measured by taking the FFT of the current that crosses the 50 Ω LISN resistor.

G is the circuit model (SPICE, SABER, etc.).

X_i for $i = (1, 2, \dots, n)$, is the i th component of the converter. In other words, the resistors, capacitors, inductors, voltage sources, and any other element are components of the converter and X_i is assigned to each one of them.

f is the frequency.

The four steps are described next.

A. Output Reduction

The first step consists of selecting a set of frequencies as follows:

$$\tilde{\mathbf{f}} = (f_1, f_2, \dots, f_m) \quad (2)$$

where f_k for $k = (1, 2, \dots, m)$ are carefully chosen values of frequency that enable one to estimate correctly an upper bound for the conducted interferences produced by G , in (1). For each f_k , one can obtain Y_k . This subset of Y s forms a vector of output variables $\tilde{\mathbf{Y}}$ depicted in

$$\tilde{\mathbf{Y}} = \begin{pmatrix} Y_1 \\ Y_2 \\ \dots \\ Y_m \end{pmatrix} = G(\mathbf{X}, \begin{pmatrix} f_1 \\ f_2 \\ \dots \\ f_m \end{pmatrix}) = G(\mathbf{X}, \tilde{\mathbf{f}}) \quad (3)$$

where $\tilde{\mathbf{Y}}$ is the set of Y_k output variables when converter G is evaluated at the frequency values given by $\tilde{\mathbf{f}}$, and \mathbf{X} is the set of all parameters X_i .

The relationship between each component of the output, denoted by Y_k , and the parameters \mathbf{X} no longer depends of the frequency, as shown in

$$Y_k = G_k(X_1, X_2, \dots, X_n) = G_k(\mathbf{X}) \quad (4)$$

where G_k is an approximate model between \mathbf{X} and Y_k in the frequency f_k , for $k = (1, 2, \dots, m)$.

B. Sensitivity Analysis

Systems described by many parameters, which correspond to a large n in (3), often contain a subset of dominant parameters. This subset can reproduce the behavior of the system with a given accuracy and with less computational effort. Moreover, it is important to find out what kind of tendency exists between the parameters and output variables, in the interval of uncertainty. Thus, the second step of the methodology is a sensitivity analysis to evaluate which parameters are actually essential and what simplified model should be used.

C. Model Reduction

Once the previous steps are completed, the converter model G in (1), with n parameters, is reduced to k simplified models depicted in

$$Y_k = G_k(\tilde{\mathbf{X}}_k) \quad (5)$$

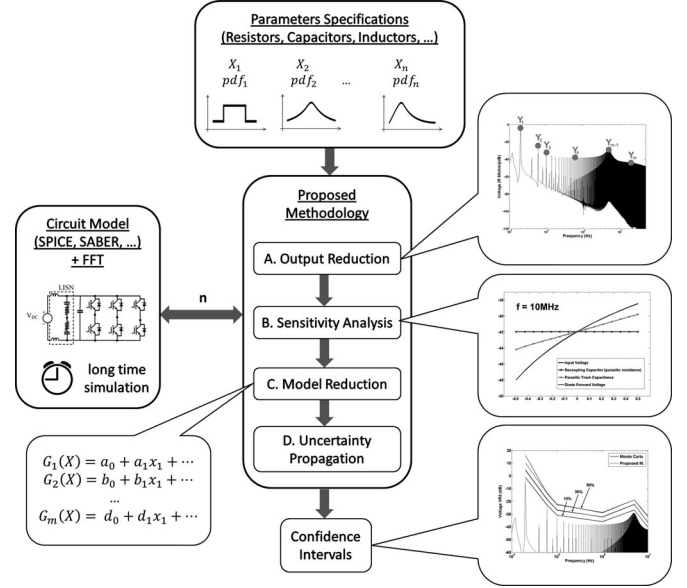


Fig. 1. Overview of the methodology.

where

G_k is the k th simplified model.

$\tilde{\mathbf{X}}_k$ is the k th subset of parameters linked to model G_k and it has dimension n_k . Considering that the parameters have different impact on the output, it is expected that $n_k < n$ for all k . Moreover, some parameters may present strong influence only in a limited frequency range.

D. Transformation of Random Variables

Finally, the last step is to determine the output PDFs by the method of cumulative distribution function [11] applied to each reduced model separately. This method allows the inputs to be distributed over any PDF.

Fig. 1 presents an overview diagram of the methodology with the steps described from A to D highlighted, in order to facilitate the comprehension of the reader. The number of calls to the circuit solver is greatly reduced compared to the MC method.

III. EXAMPLES

A. Ideal Model of a DC–DC Converter

The first example to illustrate the methodology is a model of an ideal converter with two uncertain parameters, namely the inductance and capacitance. The semiconductors, passive components, and voltage source are considered to be ideal. The output variable is the current through the inductor. Fig. 2 presents its corresponding schematic.

The nominal values of the components in Fig. 2 are given in Table I. This circuit is solved in the MATLAB SimPowerSystems environment, using the solver based on an implicit Runge–Kutta formula, described in [12] and [13].

The methodology will be applied to five different scenarios, which are described by the five PDFs shown in Fig. 3, in which the parameter nominal value is normalized to 100.

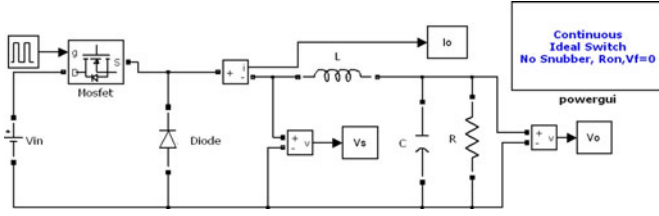


Fig. 2. Schematic of an ideal power converter.

 TABLE I
 NOMINAL VALUES OF IDEAL CONVERTER COMPONENTS

Symbol	Parameter	Value
V_{in}	Input Voltage	100 V
L	Inductance	50 μH
C	Capacitance	5 μF
R	Resistance	10 Ω
f_{sw}	Switching Frequency	20 kHz

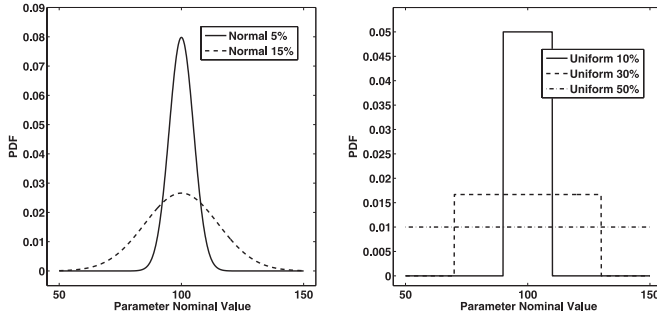


Fig. 3. PDFs of input parameter normal PDFs with 5% and 15% of standard deviation uniform PDFs with 10%, 30%, and 50% of variation around average.

The output reduction step requires a subset of frequencies which is still enough to characterize an upper bound for the output variable. One needs to choose these frequencies from the simulation corresponding to the nominal values of the components and from the impedance curves seen by the inductance L in Fig. 2, replacing the semiconductors by open- and short-circuit [14]. In this case, the circuit has no resonance.

Fig. 4 shows the simulation of the circuit for the nominal values of the parameters and one possible choice of \tilde{f} , in (2).

The sensitivity analysis provides information about which parameters influence the output the most, and which kind of model one should use to correctly represent the system. Fig. 5 presents a 3-D plot of the behavior of the output current related to the two uncertain parameters at 20 kHz. For the other selected frequencies, the shape of the output curve is similar but with different values at the corners.

Note in Fig. 5 that the slope of the curve following the inductance axis is much higher than following the capacitance axis, which means that the inductance has a stronger influence on the output. Moreover, the shape of the curve suggests that one can model it by a quadratic polynomial without crossing effects.

Thus, the model reduction step is conducted for the selected frequencies and equivalent models are computed by a general polynomial regression, using a least-squares method [15]. The

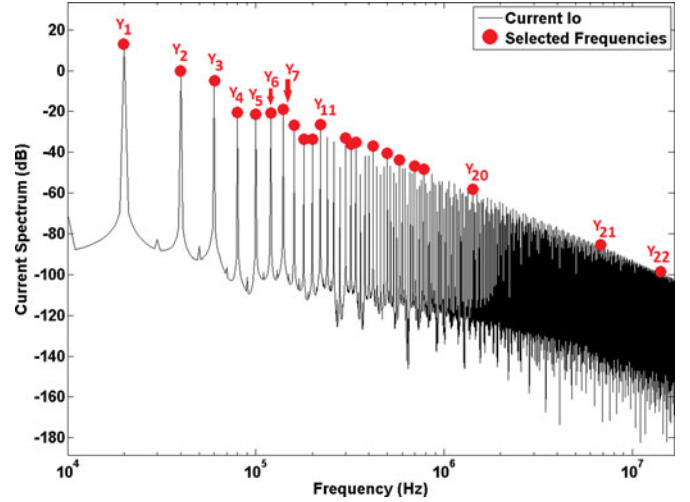
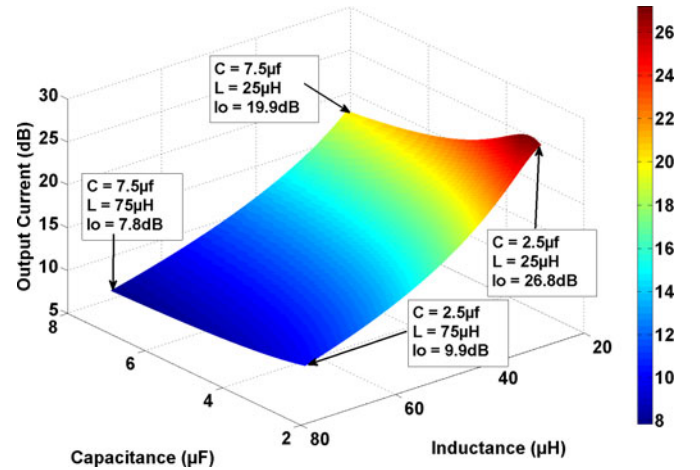

 Fig. 4. Output current I_o versus selected frequencies highlighted in red (output reduction).


Fig. 5. Sensitivity analysis (at 20 kHz).

first three fitted polynomials (G_1 , G_2 , and G_3) of the selected frequencies are shown below, with two decimal places

$$\begin{aligned}
 Y_1(C, L) &= 0.5C^2 - 1.98C + 2.87L^2 - 7.67L + 13.04 \\
 Y_2(C, L) &= 0.34C^2 - 0.55C + 1.95L^2 - 5.84L - 0.61 \\
 Y_3(C, L) &= 0.14C^2 - 0.23C + 1.74L^2 - 5.51L - 4.81 \quad (6)
 \end{aligned}$$

where

Y_k k th polynomial of the output current;

C normalized capacitance;

L normalized inductance.

The parameters were normalized so that their minimum values correspond to negative one and their maximum values correspond to positive one. In this manner, the value of the coefficient is a direct measure of the importance of a given term.

Note that the constant terms of the polynomials in (6) correspond to the value of the output current, in decibels, of the deterministic simulation shown in Fig. 4. The other terms serve to model the variation of this current with respect to parameter variation.

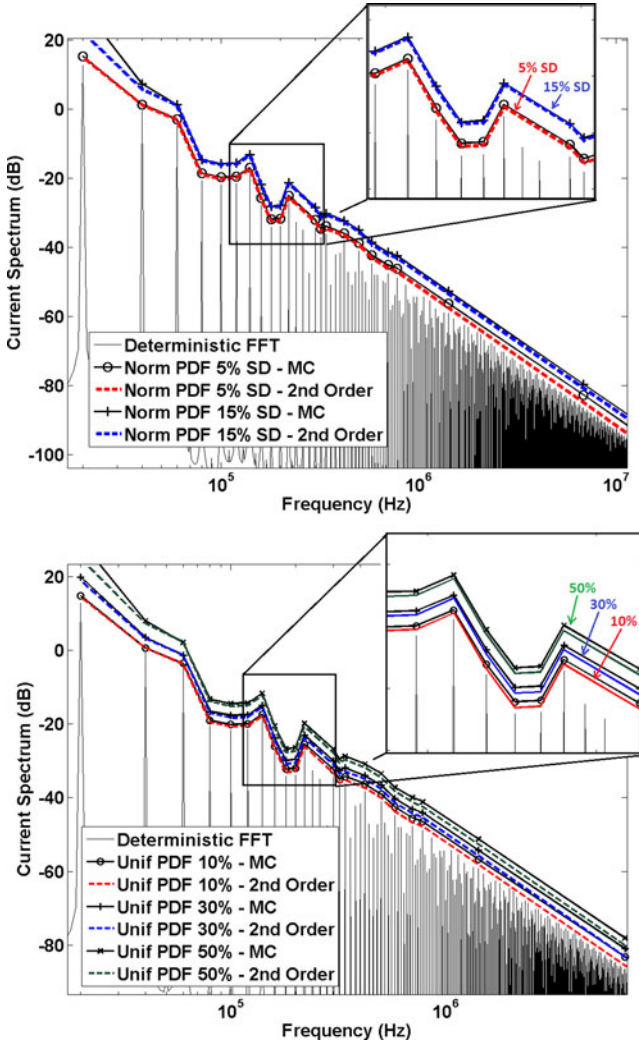


Fig. 6. Confidence intervals of the output current in decibels C and L following: a normal PDF, 5% and 15% of St. dev. (upper plot), a uniform PDF, 10%, 30%, and 50% around average (lower plot) confidence level of 0.1%.

Since these polynomials are normalized, we can immediately see that the inductance indeed affects more the output current than the capacitance. Once all models of I_o are determined, the propagation of uncertainties by transformation of random variables is efficient. The results are presented as confidence intervals in Fig. 6.

B. Ideal Model of a High-Quality DC–DC Converter

The second example to be investigated is a converter with the same topology as the one in Section III-A but with nominal values of capacitance, inductance, and resistance given in Table II. These values were chosen to illustrate how the methodology takes into account high-quality systems.

This converter has a resonant frequency at 100 kHz, which corresponds exactly to one of the harmonics generated by the switching. Fig. 7 presents the impedance measurement schematic and the modulus of the impedance.

The methodology will be applied to two of the five scenarios described in Fig. 3, which are uniform PDFs with 10% and 50%

TABLE II
NOMINAL VALUES OF HIGH-QUALITY CONVERTER COMPONENTS

Symbol	Parameter	Value
V_{in}	Input Voltage	100 V
L	Inductance	100 μ H
C	Capacitance	25.33 nF
R	Resistance	2 k Ω
f_{sw}	Switching Frequency	20 kHz

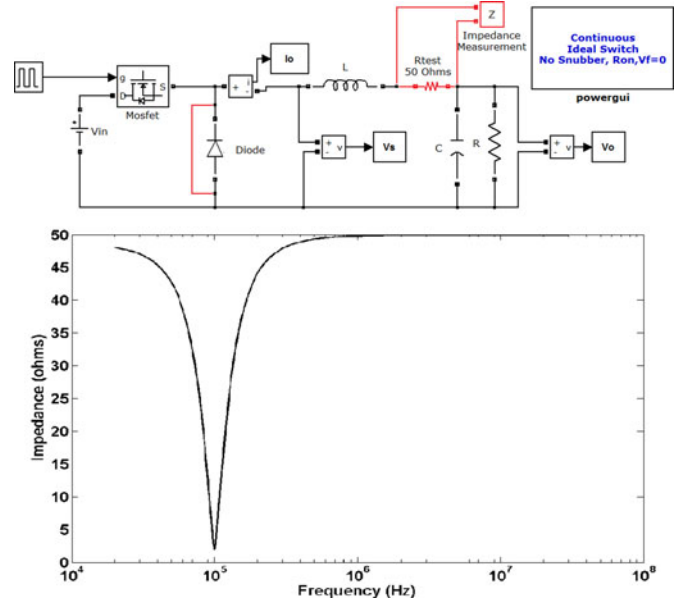


Fig. 7. Modulus of the impedance of the converter schematic with short-circuited diode and series 50 Ω test resistance.

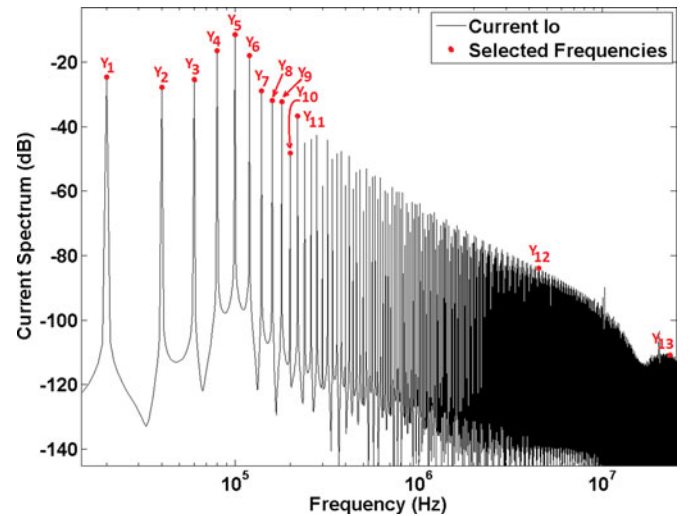


Fig. 8. Output current I_o versus selected frequencies highlighted in red (output reduction).

of deviation around average. The choice of frequencies corresponding to the output reduction step must take into account the resonant effect around 100 kHz by selecting enough points around this frequency. One possible choice is shown in Fig. 8.

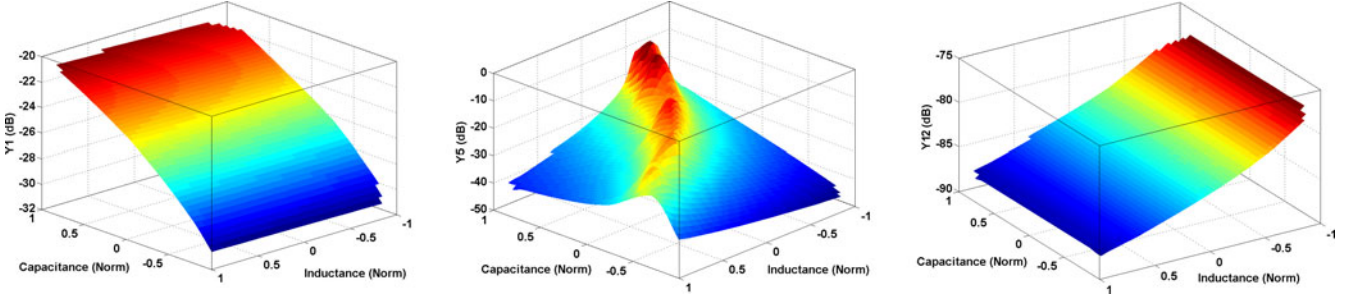


Fig. 9. Sensitivity analysis of capacitance and inductance at 20 kHz, 100 kHz, and 4.5 MHz with respect to the current I_o in decibels.

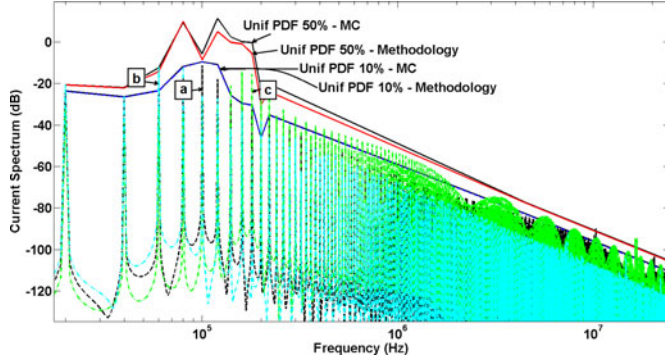


Fig. 10. Confidence intervals of the output current in decibels C and L following: a uniform PDF, 10% and 50% around average confidence level of 0.01%; deterministic plots: **a**— C_o and L_o ; **b**— $1.4C_o$ and $1.4L_o$; **c**— $0.6C_o$ and $0.6L_o$; $C_o = 25.33$ nF and $L_o = 100$ nH.

A sensitivity analysis at low, resonant, and high frequencies, which corresponds to the outputs Y_1 , Y_5 , and Y_{12} , respectively, is presented in Fig. 9. The minimum and maximum values of both capacitance and inductance are normalized. Note that at low frequency, the influence of the capacitance in the output current dominates whereas at high frequency it is the inductance the relevant parameter. Moreover, these parameters have almost linear and independent relation to the output, when they are dominant, as it is shown in Fig. 9 for the frequencies 20 kHz and 4.5 MHz.

At the resonant frequency however, both parameters must be taken into account with cross-effect terms. The data are then fitted with piecewise bicubic interpolation [16].

Once all reduced models Y_k for $k = 1-13$ are obtained, the propagation of uncertainty by transformation of random variables becomes efficient. The results are presented as confidence intervals with 0.01% confidence level, in Fig. 10.

Note that the present methodology determines upper bounds very accurately related to the MC method, for both 10% and 50% variation around the average value, and also in the range of frequency around the resonance. The indices **a**, **b**, and **c** refer to the output of deterministic simulations with a different set of capacitance and inductance values, given in Table III.

The curves of indices **b** and **c**, for instance, disrespect the upper bound of 10% parameter variation at 60 and 160 kHz, respectively. However, they respect the upper bound of 50%. These results are expected since the parameters corresponding to **b** and **c** were changed by 40%.

TABLE III
CONVERTER PARAMETERS AND RESONANCES IN FIG. 10

Index	Capacitance (nF)	Inductance (μ H)	Resonant Frequency (kHz)
a	25.33	100	100
b	35.46	140	71.5
c	15.20	60	167

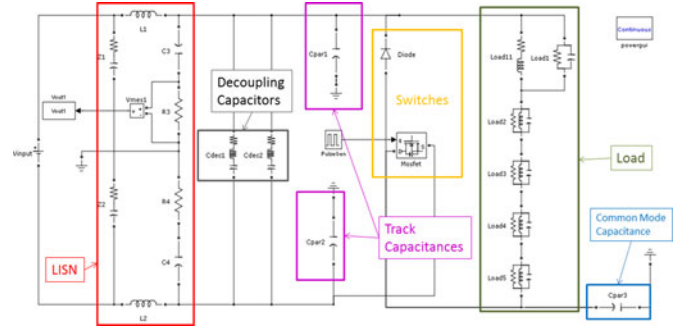


Fig. 11. Schematic of a realistic dc-dc converter.

C. Realistic Power Converter Model

The power converter model to be used in this section, as an example to test the present methodology into a more realistic model, is a dc-dc converter modeled in MATLAB/Simulink/SimPowerSystems. Fig. 11 presents the complete schematic of the converter.

The LISN is described by ten parameters while the diode and the MOSFET, for instance, are described by five and six parameters [17], respectively. The load, which is in reality an inductor, is modeled with 16 parameters in order to take into account parasitic effects at higher frequencies. The track capacitive effects are described by two capacitances and the models of the two decoupling capacitors consider the series resistance and inductance parasitic effects.

There are a total 45 parameters in this model to describe its components and their parasitic effects. This model is, thus, a realistic example of a nonlinear, time-variant power converter.

We assume the same five scenarios of parametric uncertainty shown in Fig. 3. Nevertheless, one can model these parameters by any PDF. The output variable is the FFT of the voltage in decibels across the 50 Ω resistor of the LISN. This is a standard measurement of conducted interferences. Fig. 12 shows the output considering the parameters with their average values.

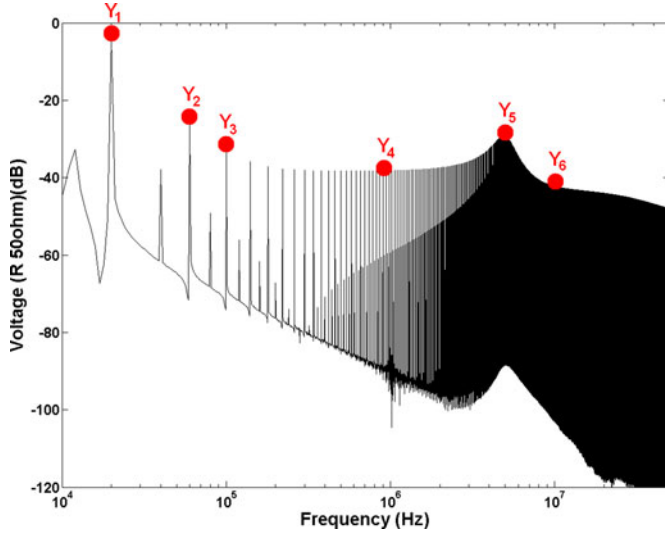


Fig. 12. Deterministic FFT of the voltage across R_3 , selected frequencies highlighted in red (output reduction).

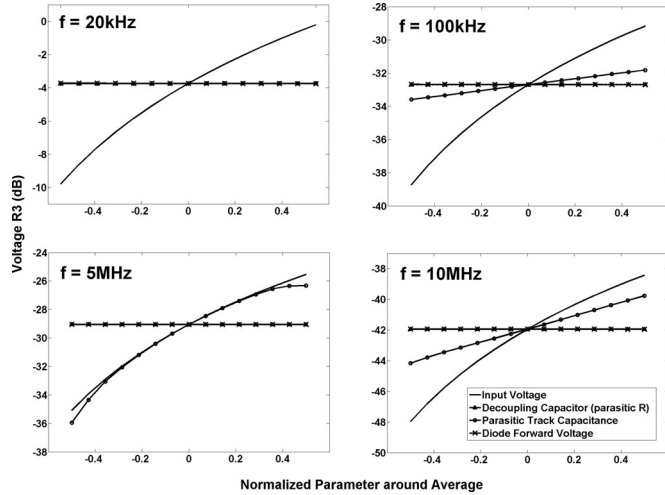


Fig. 13. Sensitivity analysis of four parameters (input voltage, ESR of decoupling capacitor, parasitic track capacitance, and diode forward voltage) at four different frequencies in the range of conducted emissions (20 kHz, 100 kHz, 5 MHz, and 10 MHz).

The deterministic output using the nominal values of components, and the lack of sharp resonances in the impedance viewed by the 50 Ω resistance, allows the choice of (0.02, 0.06, 0.1, 1, 5, 10) MHz as the frequencies to form the subset \tilde{f} in (2). This step corresponds to the output reduction.

From now on, the output is no longer the whole FFT curve shown in black in Fig. 12, but the set $Y = (Y_1, Y_2, Y_3, Y_4, Y_5, Y_6)$. This set should be sufficient to estimate an upper bound for the FFT curve.

For each element of f , we investigate the output behavior relatively to each parameter. Some of the results for a few parameters are presented in Fig. 13.

The variety of behavior along the frequency depending on the parameter analyzed is quite remarkable. For instance, the input voltage has a strong and approximately linear influence while the diode forward voltage or the parasitic resistance of

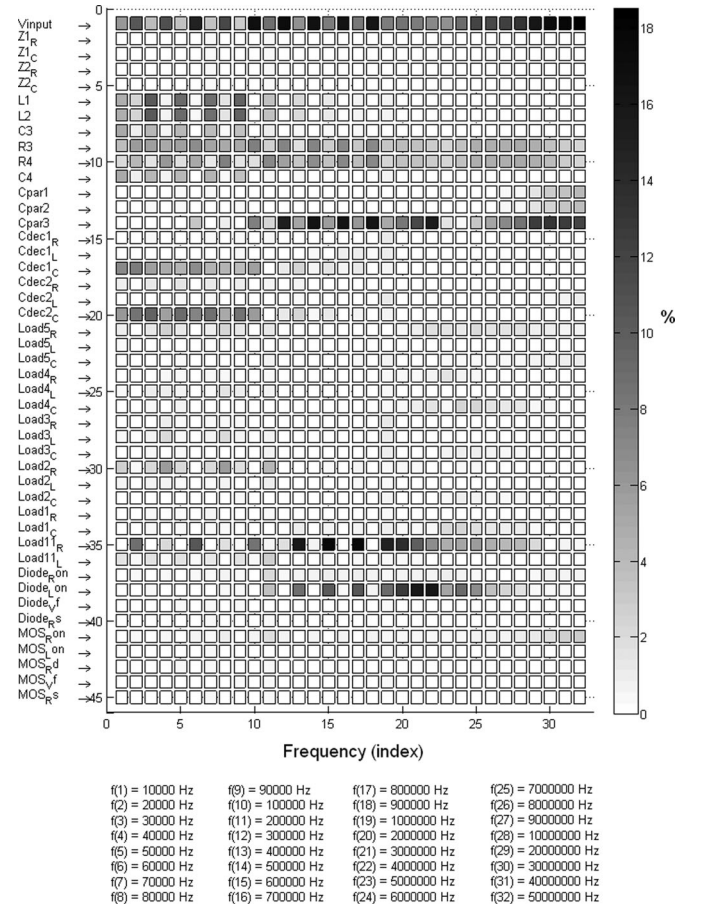


Fig. 14. Overview of parameters' impact in percentage parameters list (left column).

the decoupling capacitor has no influence at all. Moreover, the parasitic capacitance of the tracks has a frequency-dependent impact, being more relevant at the megahertz range, which is an intuitive result.

For this particular example, six second-order polynomials were sufficient as G_k for $k = (1 \text{ to } 6)$ in (5) and thereby the transformation of variables becomes a relatively simple step.

Fig. 14 presents the percentage influence of all parameters on the output, in the range of frequency which is important for conducted interferences. It is possible to rapidly verify which parameters are actually important and in which frequency range they participate.

Additionally, it is clear that there are actually a very small set of key parameters which dominate the parametric variation impact on the output. This fact is a strong motivation to apply the present methodology to problems with a large number of uncertain parameters.

Figs. 15 and 16 present a comparison of output PDFs between the MC approach with 10^4 simulations and the proposed methodology with 181 simulations, at 20 kHz, for uniform and normal distributions, respectively. Similar results were obtained for the other selected frequencies.

Figs. 17 and 18 present confidence intervals for the studied scenarios, with 99.9% confidence level. Uniform and normal PDFs are considered, respectively.

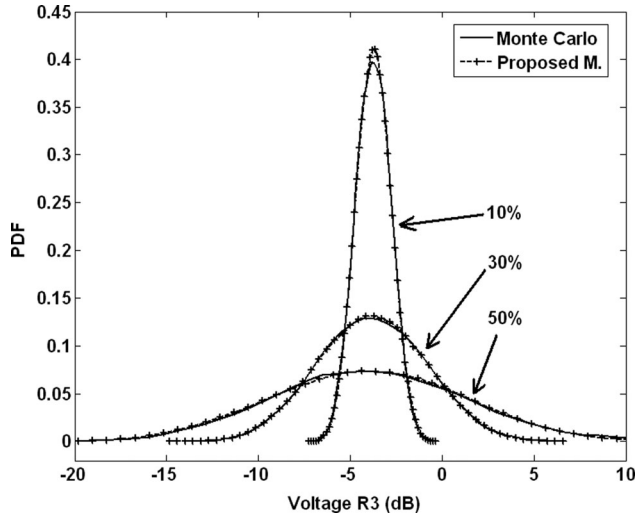


Fig. 15. Output PDFs for uniform distribution over the parameters with 10%, 30%, and 50% of margin around the average.

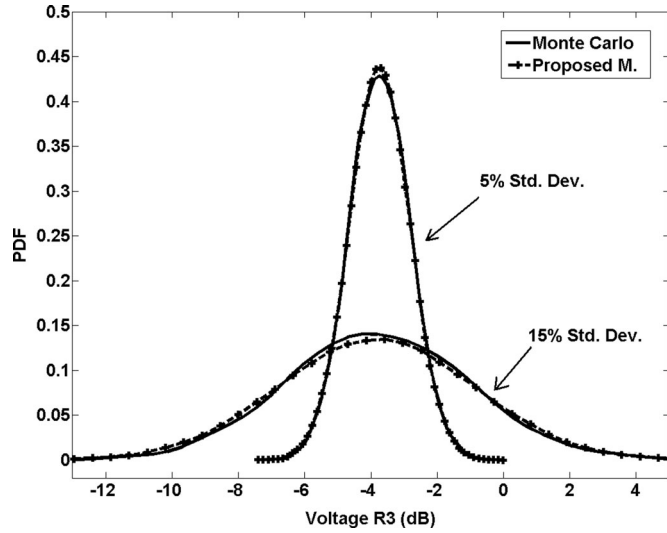


Fig. 16. Output PDFs for normal distribution over the parameters, with 5% and 10% of standard deviation.

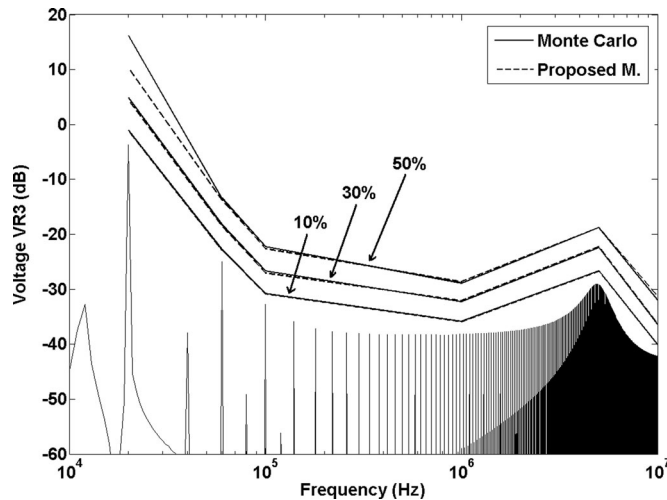


Fig. 17. Confidence intervals of voltage across R_3 uniform PDF over parameters 10%, 30%, and 50% of nominal.

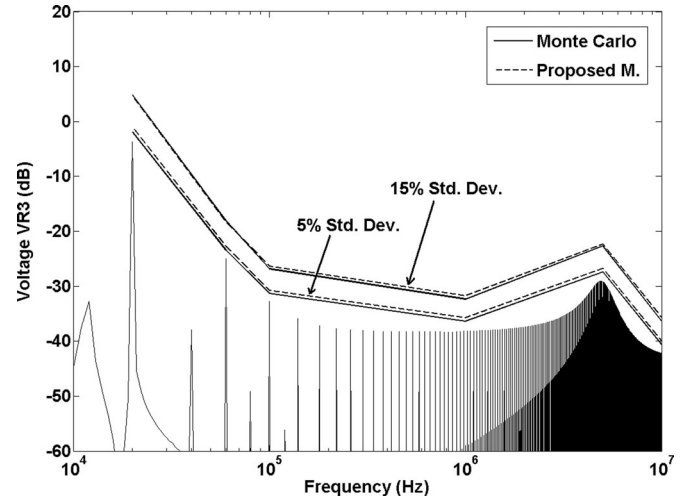


Fig. 18. Confidence intervals of voltage across R_3 normal PDF over parameters 10%, 30%, and 50% of nominal.

IV. CONCLUSION

A new methodology to quantify uncertainties in power converters from an EMC perspective has been presented. It requires far less simulations than the MC method showing similar accuracy. Moreover, the methodology was successfully tested for a nonlinear and time-variant topology of a converter with many uncertain parameters. The PDFs of the parameters can be of any kind and the output variable's PDF is computed to the desired precision, giving accurate higher statistical moments, such as skewness and kurtosis.

The present methodology is also appropriate for high-quality systems in which harmonics due to switching excite resonant frequencies. It is necessary though to consider more output variables around the sharp resonant peaks.

Finally, the results show that the upper bound for conducted interferences can be considerably higher when parametric uncertainties are present in the model if compared to a deterministic approach. Thus, the designer of power converters can make more realistic predictions at design phase in order to respect a certain EMC standard without the necessity of an unrealistic number of simulations.

REFERENCES

- [1] R. Redl, "Power electronics and electromagnetic compatibility," in *Proc. IEEE Power Electron. Spec. Conf.*, Jun. 23–27, 1996, vol. 1, pp. 15–21.
- [2] J. M. Guichon, J. L. Schanen, J. Roudet, R. Meille, and B. Revol, "Design of a PWM inverter regarding conducted EMC and losses: Influence of some key parameters," in *Proc. Ind. Appl. Conf.*, Oct. 2–6, 2005, vol. 3, pp. 1855–1859.
- [3] L. K. Warne, K. S. H. Lee, H. G. Hudson, W. A. Johnson, R. E. Jorgenson, and S. L. Stronach, "Statistical properties of linear antenna impedance in an electrically large cavity," *IEEE Trans. Antennas Propag.*, vol. 51, no. 5, pp. 978–992, May 2003.
- [4] W. S. Davies, "Monte Carlo estimates of incidence of basic access ISDN generated EMI," *Electron. Lett.*, vol. 26, no. 14, pp. 2048–2050, Jul. 1990.
- [5] S. K. Goudos, E. E. Vafiadis, and J. N. Sahalos, "Monte Carlo simulation for the prediction of the emission level from multiple sources inside shielded enclosures," *IEEE Trans. Electromagn. Compat.*, vol. 44, no. 2, pp. 291–308, May 2002.

- [6] W. S. Davies, "Monte Carlo estimates of incidence of basic access ISDN generated EMI," *Electron. Lett.*, vol. 26, no. 14, pp. 2048–2050, Jul. 1990.
- [7] E. Garcia, "Electromagnetic compatibility uncertainty, risk, and margin management," *IEEE Trans. Electromagn. Compat.*, vol. 52, no. 1, pp. 3–10, Feb. 2010.
- [8] L. R. A. X. de Menezes, A. Ajayi, C. Christopoulos, P. Sewell, and G. A. Borges, "Efficient computation of stochastic EM problems using unscented transforms," *IET Sci. Meas. Technol.*, vol. 2, no. 2, pp. 88–95, 2008. Available: http://digital-library.theiet.org/content/journals/10.1049/iet-smt_20070050
- [9] L. R. A. X. de Menezes, D. W. P. Thomas, C. Christopoulos, and A. Ajayi, "The use of unscented transforms for statistical analysis in EMC," in *Proc. Int. Symp. Electromagn. Compat., Eur.*, Hamburg, Germany, 2008, pp. 1–5.
- [10] S. I. Julier and I. K. Uhlmann, "Unscented filtering and non-linear estimation," *Proc. IEEE*, vol. 92, no. 3, pp. 401–422, 2004.
- [11] A. Papoulis and S. Unnikrishna Pillai, *Probability, Random Variables and Stochastic Processes*, 4th ed. New York: McGraw-Hill, 2002.
- [12] L. F. Shampine and M. E. Hosea, "Analysis and Implementation of TR-BDF2," *Appl. Numer. Math.*, vol. 20, pp. 21–37, 1996. Available: <http://www.sciencedirect.com/science/article/pii/0168927495001158>.
- [13] R. E. Bank, W. M. Coughran Jr., W. Fichtner, E. H. Grosse, D. J. Rose, and R. K. Smith, "Transient simulation of silicon devices and circuits," *IEEE Trans. Comput.-Aided Design Integr. Circuits Syst.*, vol. 4, no. 4, pp. 436–451, Oct. 1985.
- [14] E. Rondon, F. Morel, C. Vollaie, M. Ferber, and J.-L. Shanen, "Conducted EMC prediction for a power converter with SiC components," in *Proc. Asia-Pacific Symp. Electromagn. Compat.*, Singapore, 2012, pp. 281–284.
- [15] Available: http://www.mathworks.com/matlabcentral/fileexchange/9577_2011.
- [16] R. E. Carlson and F. N. Fritsch, "Monotone piecewise bicubic interpolation," *SIAM J. Numer. Anal.*, vol. 22, pp. 386–400, 1985.
- [17] Available: <http://www.mathworks.fr/help/toolbox/physmod/powersys/ref/f2-16412.html#f2-1837>, 2011



Moisés Ferber was born in Belo Horizonte, Brazil, on May 3, 1985. He received the B.Eng. degree in electrical engineering from the Universidade Federal de Minas Gerais, Belo Horizonte, Brazil, in 2010, where he is currently working toward the Ph.D. degree in electrical engineering at the Evolutionary Computing Laboratory in joint supervision with Laboratoire Ampère, Ecole Centrale de Lyon, Ecully, France, and G2ELab, Université de Grenoble, Grenoble, France.

His current research interests include computational electromagnetics, power electronics, electromagnetic compatibility, optimization, and uncertainty quantification.



Christian Vollaie was born in 1968. He received the M.S. degree from the University of Saint Jérôme, Marseille, France, in 1992, and the Ph.D. degree from the Ecole Centrale de Lyon, Ecully, France, in 1997, both in electrical engineering.

From 1997 to 1998, he was a Graduate Research Assistant at the Ecole Centrale de Lyon. In 1998, he joined the Laboratoire Ampère, UMR 5005 CNRS, Ecole Centrale de Lyon, Ecully, France. Since, he carries out his research with Laboratoire Ampère at the Ecole Centrale de Lyon in the field of the numerical modeling applied to the interaction between electromagnetic field of complex systems. He develops, in particular, specific formulations and numerical methods for the computation of electromagnetic fields in complex structures. One of the fields of application relates to electromagnetic compatibility.



Laurent Krähenbühl received the degree in electrical engineering from the Swiss Federal Institute of Technology, Lausanne, Switzerland, and the Ph.D. degree in electrical engineering from the École Centrale de Lyon, Ecully, France, in 1978 and 1983, respectively.

He was with Siemens (Erlangen, Germany) in 1980–1981 and with Cedrat-Recherche (France) in 1983–1985. He is currently a Senior Scientist with the Centre National de la Recherche Scientifique, Paris, France, and the Laboratoire Ampère, Ecole Centrale de Lyon, Ecully, France. His research interests include the numerical computation of electromagnetic fields (using both boundary and finite-element methods), the study of special formulations for geometrical singularities (thin layers using modified surface impedances, corners, etc.), and homogenization techniques. He is also interested in studies of complex adaptive systems, automatic design, and optimization using stochastic methods.



Jean-Louis Coulomb was born in Nîmes, France, on January 24, 1949. He received the electrical engineering degree, the "Docteur de 3^e cycle" degree, and the "Docteur d'Etat" degree from the Institut National Polytechnique de Grenoble, Grenoble, France, in 1972, 1975, and 1981, respectively.

He is currently a Professor at the Ecole Nationale Supérieure d'Ingénieurs pour l'Energie, l'Eau et l'Environnement (ENSE3), Grenoble Institute of Technology, Grenoble. He was also at the Grenoble Electrical Engineering Laboratory (G2ELab) as the Head of the Low Magnetic Fields team. His main research interest includes the electromagnetic field analysis by numerical methods with special attention to finite-element method, shape optimization, inverse problem, and software engineering.



João A. Vasconcelos received the B.Sc. degree from the Universidade Federal de Minas Gerais, Belo Horizonte, Brazil, the M.Sc. degree from the Universidade Federal da Paraíba, João Pessoa-PB, Brazil, and the Ph.D. degree from the École Centrale de Lyon, Ecully, France, in 1982, 1985, and 1994, respectively, all in electrical engineering.

He is currently a Senior Professor at the Electrical Engineering Department in the Universidade Federal de Minas Gerais, Belo Horizonte, Brazil. His research interests include single- and multiobjective evolutionary computation (optimization on design, maintenance, and operation of systems), computational electromagnetics (boundary element method, finite-element method, and moment method), and decision making.